Isothermal decompression, partial melting and exhumation of deep continental crust

DONNA L. WHITNEY, CHRISTIAN TEYSSIER & ANNIA K. FAYON
Department of Geology and Geophysics, University of Minnesota, Minneapolis, Minnesota 55455, USA (e-mail: dwhitney@umn.edu)

Abstract: Decompression of deep, hot continental crust is the primary mechanism of crustal melting, with major consequences for the geodynamics of orogens. Decompression within thickened continental crust may be initiated by processes driven from above (erosion, tectonic denudation) and/or below (crust/lithosphere thinning, buoyant rise of deep crust). On a larger scale, decompression of subducted continental crust may add material, including melt, to the overlying, non-subducting plate. This mechanism has the potential to produce large amounts of melt because fertile material is continually conveyed into the mantle, where it eventually buoyantly ascends and melts. Decompression-driven melting of continental crust may account for the high melt fractions ($\geq$20 vol.%) and great thickness (20–30 km) inferred for the partially molten layer in orogenic crust. When high melt volumes are present in the crust and/or the thickness of the partially molten layer is large, the subsequent thermo-mechanical evolution of orogens is strongly influenced by lateral (channel) and vertical (buoyant) crustal flow. For both lateral and vertical flow, the presence of melt decouples deep crust from upper crust, and continental crust from mantle lithosphere.

A major consequence of vertical crustal flow is the generation of migmatite-cored gneiss domes that riddle most orogens. High-grade rocks in many domes record pressure–temperature–time (P–T–t) paths indicating near-isothermal decompression followed by cooling from $T > 700$ °C to $T < 350$ °C in <2–5 Ma. Diapiric ascent of partially molten crust accounts for the decompression rate and magnitude required to maintain a near-isothermal path. We propose that gneiss domes are a signature of decompression and crustal melting, and are therefore fundamental structures for understanding the thermo-mechanical evolution of continental crust during orogeny.

Construction of an orogen involves crustal thickening, which occurs by tectonic shortening, addition of mantle-derived magma and/or thermal uplift of the continental lithosphere of the non-subducting plate as it interacts with the subducting/colliding plate. Crustal thickening may also occur by transfer of deeply subducted continental material from the downgoing plate to the lower crust of the non-subducting plate. During and following thickening, the nature and magnitude of thermo-mechanical links between mantle lithosphere and continental crust and between deep crust and upper crust depend in large part on the extent of partial melting of the deep crust. It is therefore important to document the location (depth), mechanisms and magnitude of crustal melting to understand the degree of coupling or decoupling between these different lithospheric layers.

Volumetrically large amounts of melt are/were present in modern and ancient orogens. Seismic and magnetotelluric data have been interpreted to indicate the presence of melt in the deep crust of young orogens (Pyrenees: Pous *et al.* 1995; Tibet: Chen *et al.* 1996; Nelson *et al.* 1996; Hirn *et al.* 1997; Central Andes and Tibet: Schilling & Partzsch 2001). Geophysical data are consistent with ~20 vol.% melt, which is likely crustally derived (Schilling & Partzsch 2001), and which may coalesce to form leucogranites (Brown *et al.* 1996). In this chapter, we explore the idea that some of the partially molten crust in collisional orogens may be derived from subducted continental material. The decompression of deeply buried or subducted continental crust is a possible mechanism for large-magnitude, near-isothermal decompression and extensive partial melting. The following are some important questions related to the origin and geodynamic evolution of partially molten crust: What mechanism(s) drive large-scale crustal melting? What are the thermo-mechanical links between continental crust in the subducting v. non-subducting plates

From: GROCOTT, J., MCCAFFREY, K. J. W., TAYLOR, G. & TIKOFF B. (eds) 2004. *Vertical Coupling and Decoupling in the Lithosphere*. Geological Society, London, Special Publications, **227**, 313–326.

of a collision zone? What is the thermal, structural and petrological fate of partially molten crust?

Partial melting of continental crust may occur by heating and/or decompression. In this chapter, we consider the evidence for and effectiveness of different mechanisms for generating melt in the deep crust. We focus on decompression because exhumed migmatite complexes – in particular, those that experienced mica dehydration melting – are commonly characterized by high-temperature, near-isothermal decompression paths and show evidence for progressive melting from high pressure (garnet stability field) to lower pressures (cordierite stability field). In addition, decompression at elevated temperatures (>700 °C) can cause dehydration melting of common crustal protoliths (e.g. mica-rich gneiss) to produce high melt fractions (e.g. Brown 1994).

The results of thermochronology and thermal modelling can be used to evaluate the conditions necessary to maintain near-isothermal conditions during decompression and to examine the thermal effects of partially molten regions that have risen from depth (>30 km) to shallow (<15 km) levels of the crust, as in the case of many migmatite-cored gneiss domes. We discuss in particular the possibility that regions of melt-bearing crust may rise buoyantly as migmatitic diapirs to form gneiss domes: domal structures cored by migmatite, orthogneiss and granitoid that occur in most orogens.

Crustal melting

A viable mechanism for melting in the deep crust must account for: (1) the amount of anatectic leucosome (≥20 vol.%) observed in many exhumed mid- to lower crustal terranes made up of migmatites and other crustally derived magmatic bodies (e.g. Brown 1994; Nyman *et al.* 1995) as well as inferred for active orogens (e.g. Schilling & Partzsch 2001); (2) the near-isothermal decompression path recorded by migmatites and other high-grade metamorphic rocks; and (3) the observation that, in the case of many upper amphibolite facies migmatite terranes, the melt has not segregated on a large scale from its source rocks. Because high-temperature decompression paths are documented for many regional-scale migmatite terranes, this chapter focuses on melting during decompression: the conditions and mechanisms of decompression, and the consequences of this process.

Melt generation

In an active orogen, partial melting of crustal rocks may occur at various stages during prograde heating by water-saturated and water-undersaturated (dehydration) melting, and/or during isothermal decompression by dehydration melting. Although water-saturated melting is commonly discounted because of the predicted low porosity (<1%) of deep crustal rocks, water-saturated melting may account for partial melting of mid-crustal terranes that are infiltrated by water-rich fluid from crystallizing plutons (Brown 1979; Montel *et al.* 1992) or deep-circulating meteoric water (e.g. Wickham 1987), particularly in cases where tonalitic or trondhjemitic leucosomes are produced from mica-bearing source rocks (Whitney & Irving 1994). In the absence of a major source of free fluid, water-saturated melting driven by release of aqueous fluids from dehydration of wet protoliths may produce low fractions (<10 vol.%) of silicic melts, assuming ~1 wt% free water and the solubility of water in crustal melts (Holloway & Blank 1994). These melts will likely crystallize soon after segregation if temperature or pressure decrease, as predicted by the negative slope of water-saturated solidi in pressure–temperature (P–T) space. Vapour-absent (dehydration) melting can, however, produce greater amounts of granitic melt (20–60 vol.%; Clemens & Vielzeuf 1987; Vielzeuf & Holloway 1988) that may remain largely uncrystallized during ascent of the melt or decompression of the melt and host rock.

Within a region, the melt fraction produced during dehydration melting is a function of the bulk composition of rocks that reached P–T conditions sufficient for melting, and the volume of fertile rock. Reaction curves for biotite dehydration melting have a steep slope, and so are encountered by P–T trajectories during steep decompression or during heating and initial decompression (Fig. 1). Once the solidus is crossed, paths tend to be subparallel to the solidus, on the melt-present side, perhaps owing to a combination of thermal buffering by the melt and dynamic effects of melt-enhanced decompression (discussed in later sections). The melt will not crystallize until it reaches much lower pressures because of the steep dP/dT slope of the solidus. Melting may also occur during the late stages of decompression as water is released from crystallizing melts, creating conditions for water-saturated melting (Thompson 2000).

Melt segregation: mechanisms and scales

The observation that migmatite terranes contain large fractions (20–40 vol.%) of crystallized

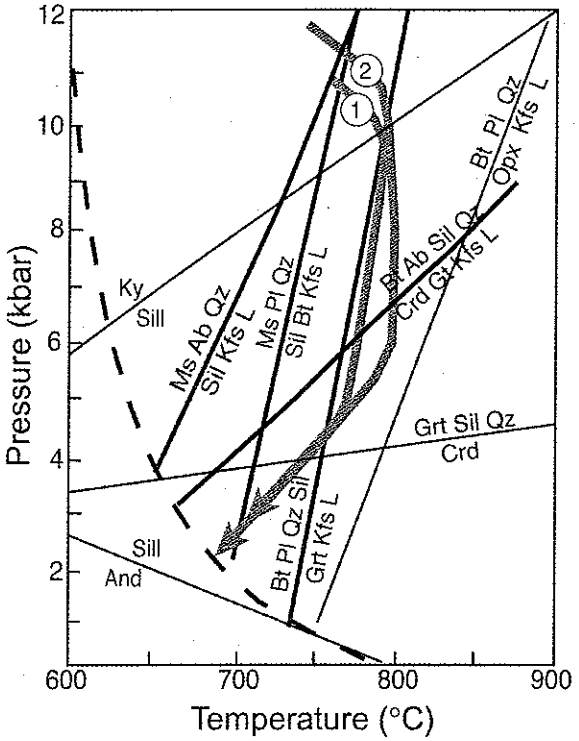

Fig. 1. Pressure–temperature–time paths showing near-isothermal decompression of: (1) Thor-Odin gneiss dome, Shuswap complex, British Columbia (Norlander *et al.* 2002); and (2) South Brittany migmatite terrane (Audren & Triboulet 1993). Various reference solidi are shown: water-saturated melting of a metapelitic rock (dashed curve); dehydration melting of muscovite gneiss (end-member muscovite + albite, and muscovite + intermediate plagioclase); and dehydration melting of biotite gneiss. Although shown as a line in the figure, biotite dehydration melting defines a region in P–T space, owing to solid solution in biotite. Most migmatite terrains and gneiss domes did not exceed the upper stability of biotite + plagioclase + quartz, as indicated by the lack of orthopyroxene. Because some migmatites/gneiss domes show evidence for late, low-pressure, high-temperature growth of cordierite, two equilibria involving cordierite are also shown (one solidus, one subsolidus).

silicic melt that has segregated on a centimetre scale but has not drained far from its source has fuelled a long debate about the connection, or lack thereof, between anatectic migmatites and granitoids (Brown 1994, and references therein). Much attention has been given to determining small-scale melt-segregation mechanisms and discussing how silicic melt, once segregated from its source, might flow, coalesce and pool to form larger-scale magma bodies, such as orogenic leucogranites (Le Fort *et al.* 1987; Inger & Harris 1993). Possible mechanisms contributing to segregation and transport include compaction (McKenzie 1984) and flow through dykes/fractures (Clemens & Mawer 1992), shear zones (Brown & Solar 1998), or channels (Sawyer 2001).

Most of these segregation/transport models involve consideration of how melt separates from its source and disperses. In the discussion below, we consider the implications for crustal dynamics of melt *not* leaving the system: that is, melt is segregated only on a local scale (1 cm to 100 m) and remains largely within the source rocks. Although some melt may escape, enough is retained for the migmatite complex to be buoyant. In this case, the most significant motion is not of the melt itself relative to its source (matrix), but of melt and matrix relative to less molten/more dense rocks. The generation and partial retention of melt may strongly influence the subsequent P–T path and dynamics of the partially molten rocks. We next consider mechanisms that could produce decompression melting of continental crust, before further discussing the implications for the thermo-mechanical evolution of orogens.

Near-isothermal decompression paths and mechanisms

In thickened orogenic crust, the movement of high-grade metamorphic rocks from the mid- to lower crust towards the Earth's surface commonly occurs at near-isothermal conditions for a few to $\geq$10 kbar of decompression ($\geq$33 km) (Fig. 1). In some terranes, decompression may be preceded or accompanied by heating. High-temperature decompression paths have been demonstrated for migmatite terranes (e.g. Jones & Brown 1990; Whitney 1992; Audren & Triboulet 1993), including migmatite-cored gneiss domes (Norlander *et al.* 2002), and other high-grade rocks, including some ultrahigh-pressure terranes (e.g. Su-Lu, China: Wang *et al.* 1993; Western Gneiss Region, Norway: Dunn & Medaris 1989). P–T paths estimated for many exhumed high-grade metamorphic rocks as well as those calculated by forward modelling for the thermal evolution of thickened crust (England & Thompson 1984) remain within ~50–80 °C of T_{max} during a substantial portion of the decompression path. These temperatures are within the uncertainty range of most metamorphic temperature calculations (e.g. geothermometry based on cation exchange), so it is not possible to discern details of the paths other than that they remain at high temperature during decompression.

For average values of thermal conductivity, mantle heat flux, crustal heat production and other factors related to deformation and metamorphic reactions, isothermal decompression is not

predicted by thermal models for slowly eroding (<1 mm a^{-1}) orogens unless there is a gap in time ($\sim$10–30 Ma) between maximum crustal thickening and unroofing. This gap permits the generation of radiogenic heat from buried crust and relaxation of isotherms. For orogens with little or no gap in time between thickening and denudation/decompression, elevated temperatures can be maintained during decreasing pressure if decompression is rapid ($\gg 1$ mm a^{-1}). In the following sections, we consider different decompression mechanisms (Fig. 2) and discuss whether each is likely to be a significant factor in maintaining elevated temperatures during decompression. We focus on mechanisms that account for decompression on a regional scale with magnitudes of >10 km (and, in some cases, tens of kilometres), such as commonly observed in migmatite complexes, gneiss domes and ultrahigh-pressure metamorphic terranes, so that we can better understand thermomechanical links and feedback relationships among orogenic processes operating at the surface, at different levels within the continental crust and within the mantle.

Erosion

Unroofing via erosion may account for large-magnitude isothermal decompression if the erosional products are removed from the system or if there is a large lag time (>10 Ma) between crustal thickening (deep burial) and the initiation of denudation. In the latter case, high-temperature decompression and partial melting may occur in part because of the added crustal heat production from buried radiogenic crust, following crustal thickening (England & Thompson 1986). Rapid erosion (≥ 1–5 mm a^{-1}) in concert with tectonism (uplift, faulting; Fig. 2a) may account for localized decompression, such as beneath alpine glaciers and deeply incised rivers (e.g. Zeitler *et al.* 2001), although, in the latter case, many questions remain about how rivers or river systems evolve (move) through time and influence exhumation over a region much greater than that of the main incised channel. For regional-scale, large-magnitude decompression of deep crust, it is likely that other mechanisms are responsible for near-isothermal decompression, particularly in orogens in which there was no lag time between crustal thickening and thinning/decompression.

Low-angle normal faults

Detachment systems can lead to exhumation/decompression of deep-seated rocks by crustal thinning during symmetric or asymmetric extension (Lister & Davis 1989). For example, asymmetric detachment systems may create a locus of lower crust upwelling that is offset relative to the normal fault break-away zone. Melting during this initial decompression is likely; however, given the low angle of the detachment, rocks cool as they are exhumed in the footwall of the detachment system, and therefore do not experience isothermal decompression (Fayon *et al.* 2002). Therefore, detachment faults are unlikely to account for the magnitude of decompression observed in gneiss domes and other high-pressure terranes unless the faults were originally higher angle (Buck 1988) or the rate of motion on detachments is unusually fast.

Crustal thinning/collapse

Regional crustal thinning may drive decompression of the deep crust during collapse of thickened crust (Rey 1993) (Fig. 2b), especially if thinning is localized in a narrow region. Thinning may involve the upper crust, lower crust, or both. Decompression by thinning of thickened crust and lateral flow of deep crust is slow if thinning is restricted to the lower crust, but can be significantly faster if the upper crust is extended, thinned and/or rapidly eroded (Teyssier & Whitney 2002). Because the rate of bulk thinning likely decays with time; this mechanism may initiate decompression, but acting alone it is unlikely to maintain near-isothermal conditions during substantial decompression. Crustal thinning combined with buoyancy may, however, produce the observed and modelled pressure–temperature–time (P–T–t) paths.

Folding/buckling

Folding of the lithosphere under compression has been shown to occur in oceanic lithosphere (Wiessel *et al.* 1980; Gerbault 2000), and possibly also in continental lithosphere (Martinod & Davy 1994; Burg *et al.* 1994). Buckling theory predicts the amplification of folds of a particular wavelength, given appropriate viscosity contrasts and layer thicknesses. As an antiformal buckle develops (Fig. 2c), a positive feedback relation between folding and erosion may cause an acceleration of fold amplification, resulting in effective, localized lithospheric uplift. This principle has been applied to the exhumation of metamorphic rocks in the Namche–Barwa syntaxis of the eastern Himalayas (Burg *et al.* 1997). The combined effect of fold amplification and erosion may allow exhumation under near-isothermal conditions, such as the P–T path

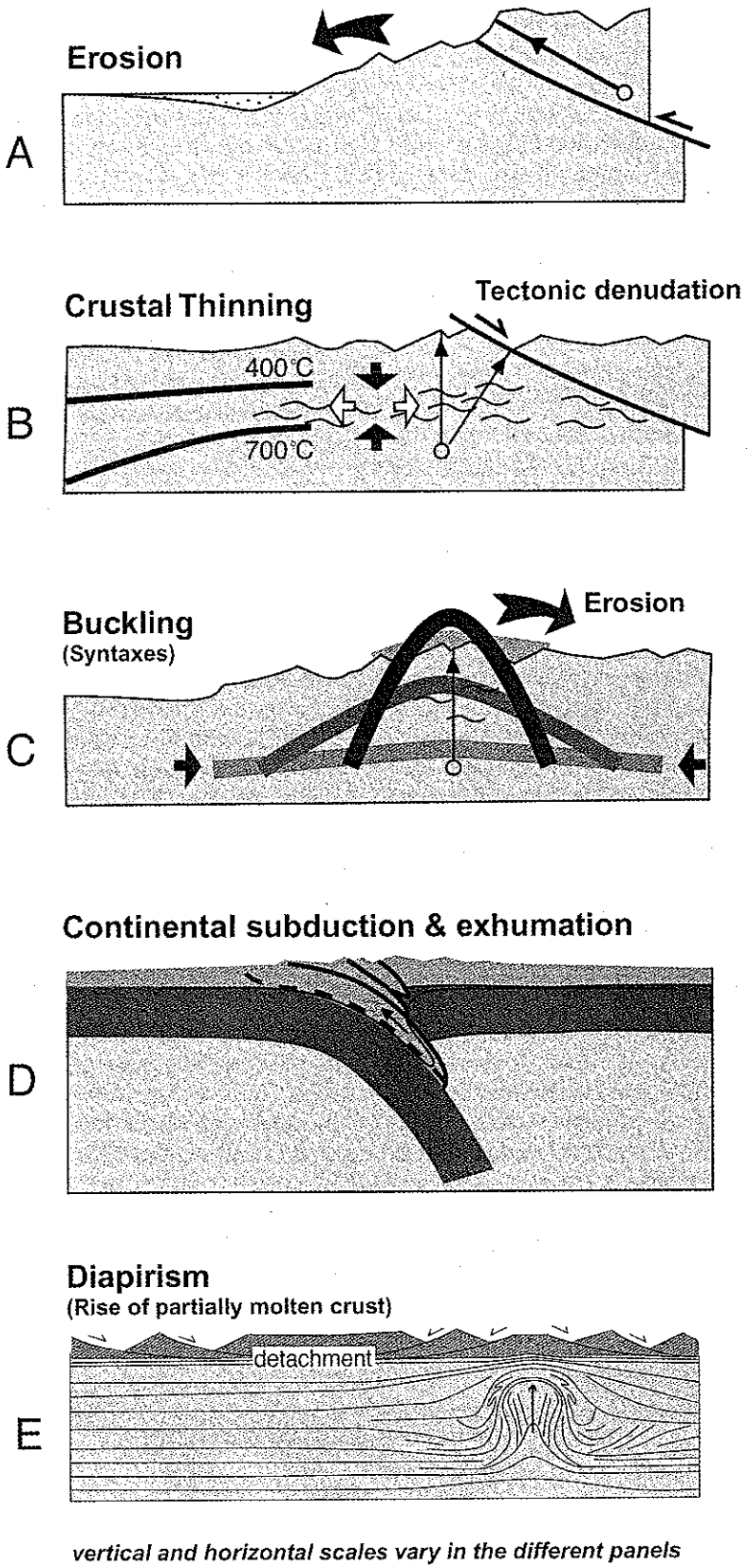

Fig. 2. Some of the decompression mechanisms described in the text (**a**) erosion of uplifted rocks (may be coupled with local faulting/crustal shortening); (**b**) crustal thinning associated with normal faulting (also shown are schematic 400 and 700 °C isotherms and a partially molten mid-crustal zone); (**c**) crustal buckling (e.g. at orogenic syntaxes); (**d**) exhumation of subducted continental crust; and (**e**) upwelling of a partially molten diapir with associated downflow of denser rocks (upwelling may be driven by density inversion or triggered by removal of the upper crust or thinning of the deep crust).

inferred for metamorphic rocks at the Namche–Barwa and Nanga–Parbat syntaxes (Burg & Podladchikov 2000). Buckling may therefore be an effective mechanism of localization of lithospheric uplift. If this lithospheric uplift is accompanied by fast glacial and/or fluvial erosion, heat will be advected upward and a positive feedback relation between crustal softening and strain localization will occur and lead to localized, near-isothermal decompression.

Exhumation of ultrahigh-pressure rocks (continental subduction)

Continental subduction provides a means of burying and heating a large volume of fertile material that is continually being replenished as long as subduction is active. This mechanism can produce large volumes of melt in orogens, and results in the most dramatic examples of large-magnitude decompression of continental material. Ultrahigh-pressure (UHP) terranes represent continental material that has been subducted to depths of >100–150 km and exhumed, as shown by the presence of coesite and diamond in metamorphosed supracrustal rocks (Chopin 1984; Coleman & Wang 1995).

The largest-magnitude *isothermal* decompression in continental orogens is recorded by UHP terranes (e.g. Zhang *et al.* 1997; Nakamura & Hirajama 2000). UHP terranes now exposed at the surface typically represent crustal slices exhumed at/near the suture zone, and some are in fault contact with blueschist and serpentinite complexes (Dora-Maira, Western Alps; Dabie Shan, China). The subducted crust that returns to the surface as an identifiable UHP terrane may have remained close to the subduction zone and been exhumed via buoyancy-driven exhumation of a slice bounded below by a thrust and above by a normal fault (Chemenda *et al.* 1995) (Fig. 2d). Subducted continental crust that does not experience a return path near the suture may remain accreted to the base of the overriding plate as slices of continental crust and lithospheric mantle, or may be added to the base of orogenic crust during melting of buoyantly ascending crustal material. Highly oblique subduction, such as proposed for the subducting continental lithosphere under Tibet (Tapponnier *et al.* 2001), may facilitate prolonged burial/heating and delayed exhumation, creating the right thermal conditions for melting during ascent (Fig. 3).

Active collisional orogens provide information about the scale of continental subduction. For example, geophysical studies of subcrustal structure beneath the Himalayan orogen show that a zone of low-density material resides beneath Tibet as well as the western Himalayas (Nelson *et al.* 1996; Van der Voo *et al.* 1999). This zone comprises in part continental crust from the subducted Indian plate (Zhao *et al.* 1993), as well as subducted continental material from the Eurasian plate (Tapponnier *et al.* 2001). In the western Himalayas–Hindu Kush–Pamir zone of central Asia, geophysical evidence documents ongoing steep subduction of continental lithosphere, including low-density crustal rocks (the Indian continental margin). In this region, earthquake hypocentres (Searle *et al.* 2001) and tomographic images based on P-wave velocities (Van der Voo *et al.* 1999) show a steeply dipping region of continental lithosphere that has descended into the mantle to ~300 km depth. To the east, under southern Tibet, Indian lithosphere is currently subducting at a shallow angle (Zhao *et al.* 1993; Owens & Zandt 1997). Evidence from active and ancient orogens

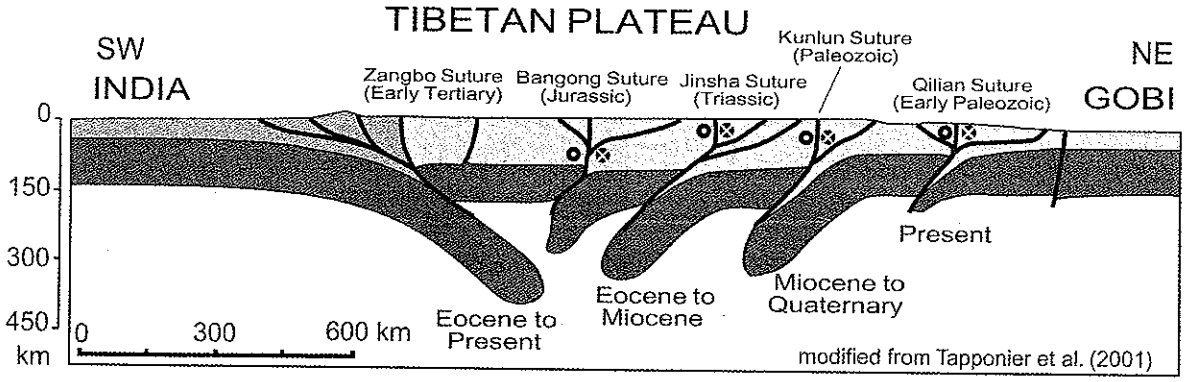

Fig. 3. Tectonic model for continental subduction, decompression and partial melting. Advanced subduction of continental material along multiple, sequential subduction zones (now sutured). Modified from the model of Tapponnier *et al.* (2001). The oldest subducted continental material has risen buoyantly, melted and contributed to crustal thickening of the Tibetan Plateau.

suggests that continental subduction is a major process in the evolution of orogens, and that exhumation of subducted continental rocks may be isothermal at high temperatures. The role of melting in this process remains to be discussed (see following section on 'Partial melting in orogens').

Buoyancy/diapirism

Lower-density rocks underlying higher-density rocks may rise buoyantly if rheological properties allow flow. During orogeny, a regional-scale density inversion can be achieved in several ways: (1) tectonic stacking of terranes/thrust slices that are more dense than underlying felsic basement; (2) subduction of continental crust into the mantle; and (3) reduction in bulk density of rocks by addition of felsic magma, with no large-scale segregation of melt. One or more of these situations, combined with the fact that rocks are generally weak at depth owing to elevated temperature and the presence of even small amounts of melt, creates a condition for gravitational instabilities to develop and grow (Fig. 2e). For the case of schist/gneiss overlying granitic basement, the density contrast ($\sim$0.1–0.3 g cm^{-3}) is sufficient for solid-state diapirism (Fletcher 1972; Soula *et al.* 2001).

The magnitude of decompression of rising diapirs may be significant, as flow is along subvertical trajectories for a significant portion of the ascent. Once initiated, diapirism may be self-sustained by a positive feedback relation between decompression and melting. The presence of melt lowers the bulk density within the diapir relative to its surroundings, enhancing upward flow and decompression. Rise of partially molten crust is accompanied by downflow of surrounding rocks, which may be transformed to granulite and eclogite that accumulate in the lower crust.

The rate of decompression of deep crustal rocks by buoyancy-driven flow will be higher if diapirism is coupled with thinning of thickened crust, particularly if the upper crust is removed by extension, tectonic denudation and/or erosion. The rising diapir may localize upper crustal extension, or the removal of upper crust may drive the buoyant rise of partially molten crust. It is likely that these processes are coupled because they involve a positive feedback relation through the generation of melt (Teyssier & Whitney 2002). The rise of diapirs comprising partially molten crust can account for large-magnitude, near-isothermal decompression if the rate of ascent is fast enough to maintain elevated temperatures and some melt remains in the system.

Partial melting in orogens: mechanisms and consequences

Two major processes that characterize collisional orogens are crustal melting and the exhumation of formerly deep continental material. These processes may be genetically linked, as demonstrated by the P–T–t histories of migmatite complexes, and in particular migmatite-cored gneiss domes that are observed in exhumed orogens worldwide.

Migmatite diapirs and gneiss domes

In orogens, the geological expression of partially molten crust that has experienced high-temperature, near-isothermal decompression is commonly a migmatite-cored gneiss dome. Gneiss domes occur in orogens ranging in age from Archaean through Cenozoic and in tectonic setting from wide (hundreds to thousands of kilometres wide) orogens to narrow (<10 km wide) shear zones. Well-documented examples occur in the North American Cordillera, Himalayas (Zanskar, Karakorum, Garwhal, South Tibet), Pamirs, Alps (central Alps, Aegean region, Anatolia), Iberian and French Variscides, the Bering Sea region (Alaska, Russia), and the Appalachians, as well as numerous domes in Precambrian terranes.

Typically, more than one dome is present in a region, they are elongate and aligned parallel to the strike of the orogen, and they are characterized by a core of anatectic migmatites, orthogneiss and/or granitoids surrounded by high-grade metasedimentary rocks. In some orogens, there is a characteristic spacing between gneiss domes, e.g. 40–50 km in the northern Cordillera, and 25 $\pm$ 5 km in the northern Appalachians (Fletcher 1972). The short dimension of gneiss domes ranges from $\sim$4 km (Naxos, Greece; Baltimore, USA) to 60 km (Velay, Massif Central, France), but most domes have a short diameter of 15–25 km.

The origin of gneiss domes has been debated for more than 50 years (Eskola 1949). Their origin has been ascribed to diapirism (Berner *et al.* 1972; Ramberg 1980; Calvert *et al.* 1999), crustal shortening (Ramsay 1967; Burg *et al.* 1984; Rolland *et al.* 2001), extension (Chen *et al.* 1990; Brun & Van Den Driessche 1994; Escuder Viruete *et al.* 2000), or more complicated models invoking both contraction and extension (Lee *et al.* 2000),

crustal flow/extrusion (Beaumont *et al.* 2001), or extension-controlled upwelling of partially molten crust (Vanderhaeghe *et al.* 1999). In recent years, diapirism has been rejected as a general mechanism for the generation of gneiss domes because in many cases the structural doming event is believed to post-date partial melting/magmatism (e.g. Lee *et al.* 2000; Rolland *et al.* 2001).

In most orogens, the crustal structure beneath gneiss domes is not known, but in southern Tibet, seismic profiles suggest that the partially molten (high conductivity, low seismic velocity) mid-crust extends to the base of the Kangmar dome (Nelson *et al.* 1996). Recent papers have suggested links between the deep crust of the southern Tibet and the Himalayan wedge, including flow of ductile Tibetan crust into the Himalayan wedge (Beaumont *et al.* 2001; Grujic *et al.* 2002).

An example of the relationship between decompression and doming is found in the Shuswap metamorphic core complex, British Columbia, where a series of elongate gneiss domes are aligned along the strike of the belt near its eastern margin. These domes are approximately 15 km across their short axis, are located ~40–50 km apart, and include the Frenchman's Cap, Thor-Odin, Pinnacles and Valhalla domes. The high-grade core of the Thor-Odin dome experienced near-isothermal decompression from $P \geq 10$ kbar to $P < 4$ kbar (Norlander *et al.* 2002). The dome is defined in part by the transition from migmatitic rocks that retain a coherent metamorphic layering, to migmatites dominated by the granitic fraction and characterized by lack of a coherent solid framework (Vanderhaeghe *et al.* 1999).

Isothermal decompression of migmatite domes

The advection of partially molten material from >30 km depth towards the Earth's surface is a significant agent of heat transfer during orogeny. The temperature–time history at shallower levels depends on the final emplacement depth of the diapir and the geothermal gradient of the upper crust: these are controlled by surficial processes and upper crustal deformation (e.g. extension, erosion). Thermal modelling can be used to evaluate the conditions required for near-isothermal decompression and to examine the thermal effects of migmatite diapirs following ascent to the upper crust.

We used time-dependent thermal modelling to quantify the relationship between isothermal decompression of a diapir and cooling rates (Fig. 4). The advection–diffusion equation is solved in two dimensions using an explicit finite-difference method (e.g. Noye 1982). These models illustrate the thermal response of a diapir rising from the deep crust to the middle crust and do not address the mechanical issues of emplacement of diapirs into the rigid upper crust. Despite the mechanical limitations, important information regarding the relationship between pressure–temperature (P–T) and temperature–time (T–t) paths is obtained through this analysis. The predicted T–t paths (Fig. 5) can be compared to observed paths (Fig. 1) to evaluate the exhumation history.

The diapir is modelled as a piston 15 km wide with an initial temperature of 775 °C (Fig. 4a). The diapir ascends from a depth of 30 km at a constant rate to mid-crustal levels. Points within the diapir are advected vertically; exhumation rates investigated by the model were 2, 5, 10, 15 and 20 km Ma^{-1}. The more rapid rates are consistent with rates recorded by rocks exposed in migmatite-cored domes (e.g. Brown & Dallmeyer 1996; Calvert *et al.* 1999). The initial geothermal gradient is non-linear, with an increase in temperature from 320 °C at 15 km to 550 °C at 16 km. Below this interval, which represents the base of a rigid upper crustal lid, the geothermal gradient changes to 10 °C km^{-1}. The results shown in Fig. 4 illustrate the effects of the diapir stopping at the base of the upper crustal lid (Fig. 4b) and piercing the upper crustal lid (Fig. 4c).

Pressure–temperature–time paths calculated for various points within the diapir, according to the second model (the diapir pierces the upper crust) and an exhumation rate of 20 km Ma^{-1}, are illustrated in Fig. 5a. These results show that, even at extreme exhumation rates, a rock at the top of the diapir (initial depth = 30 km) loses heat to the surroundings during decompression, and therefore records cooling during decompression. In contrast, rocks within the diapir (initial depth = 35 or 39 km) retain heat for a longer period of time during decompression, resulting in a component of near-isothermal decompression. The numerical experiments therefore predict that rocks within a diapir initiating within the deep crust maintain significantly high T (>700 °C) during decompression to shallow mid-crustal levels. Once the diapir is emplaced at a shallow level, the associated cooling paths predict a range of cooling rates from 24 °C Ma^{-1} to as high as 400 °C Ma^{-1} (Fig. 5b). Both models shown in Fig. 4b and c predict greatest cooling rates of 400 °C Ma^{-1} during exhumation for rocks at

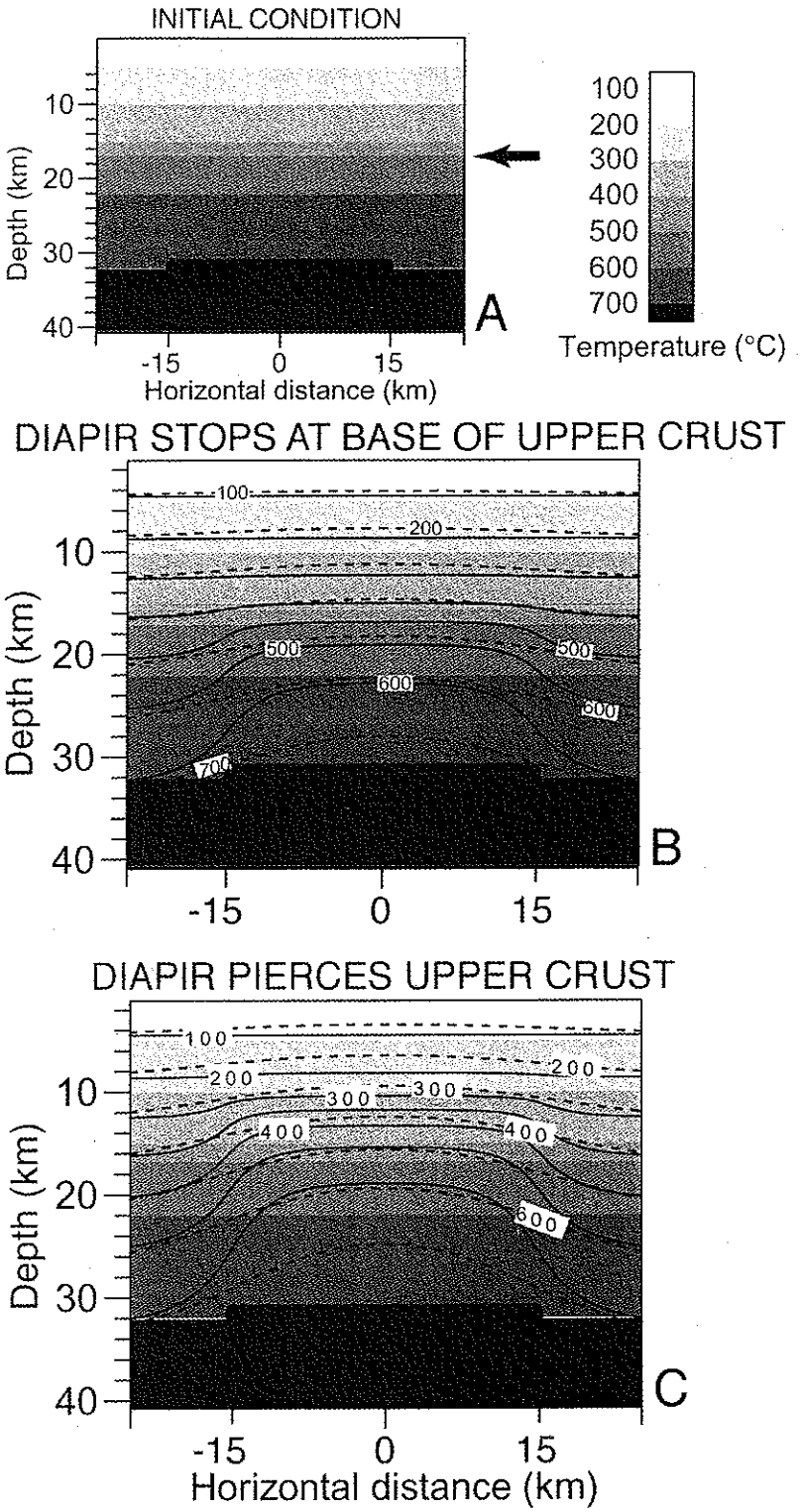

Fig. 4. (**a**) Initial conditions for time-dependent numerical experiments. The initial geothermal gradient is determined using a heat production value of 9.6×10^{-4} μW kg^{-1} for the upper crust and 5×10^{-5} μW kg^{-1} for the lower crust. The boundary between the upper and lower crust is located at 15 km (arrow). The diapir is modelled as a piston, the top of which is initially at 30 km depth and moves vertically at a given rate. $T_{initial}$ for points within the piston is 775 °C. Boundary conditions are constant basal heat flux and constant surface temperature, $T_{surf} = 20$ °C. (**b**) Diapir is exhumed to the base of the upper crust at 20 km Ma^{-1}. Dashed contours show position of isotherms after advection (1 Ma); black contours represent thermal structure after 5 Ma of cooling at $t = 6$ Ma. Contour interval = 200 °C. (**c**) Diapir is exhumed to a position within the upper crust at a rate of 20 km Ma^{-1}. Contours are the same as in (**b**). In both models, rocks near the top of the diapir record the greatest cooling, but the magnitude of cooling is greater in the case where the diapir pierces the upper crust.

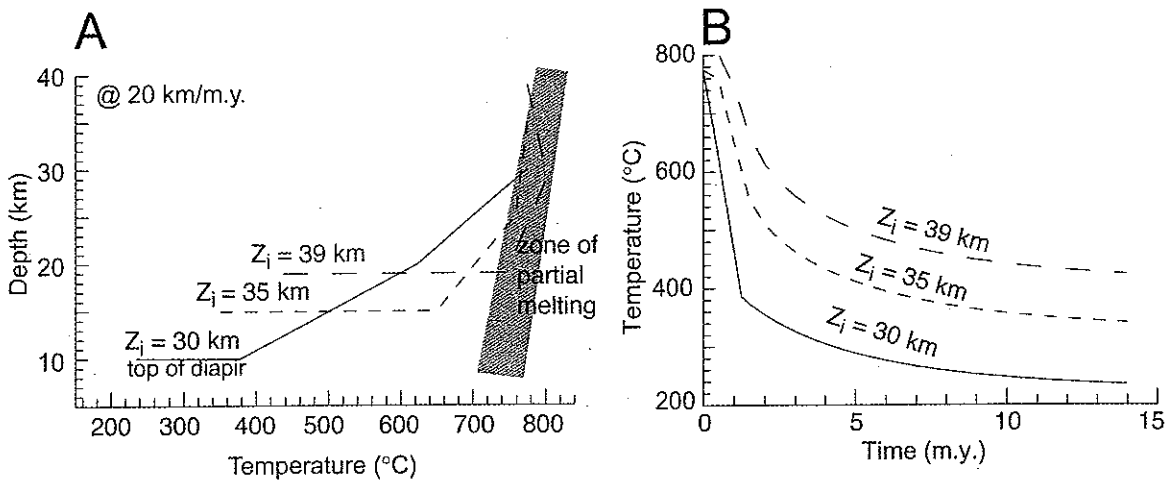

Fig. 5. (**a**) Depth (pressure)–temperature diagram showing model results for a particle point located at the top of the diapir (initial depth, $Z_i = 30$ km), a point 5 km below the top of the diapir ($Z_i = 35$ km) and a point 9 km below the top ($Z_i = 39$ km). The decompression rate for all three cases is 20 km Ma^{-1}. The top of the diapir cools continuously during decompression, but the points modelled within the diapir experience near-isothermal decompression until the diapir pierces the upper crust, at which point the diapir experiences isobaric cooling. The grey shaded region illustrates the approximate location of dehydration melting reactions involving biotite. (**b**) The T–t plot corresponding to the same conditions as in (**a**) with similar labels and line styles. This T–t diagram illustrates the rapid cooling rates of the modelled processes.

the top of the diapir. Following exhumation, the cooling rate slows to 24 °C Ma^{-1}. The average cooling rate recorded for a rock at the top of the diapir is 56 °C Ma^{-1}. A rock within the diapir, however, records a slower average cooling rate of 40 °C Ma^{-1}. These cooling rates are consistent with observed cooling rates determined by thermochronology of migmatite-cored domes (e.g. Calvert *et al.* 1999; Vanderhaeghe *et al.* 1999).

Observed P–T–t paths for migmatite-cored domes suggest rapid isothermal decompression of the deep crust. Calculated P–T–t paths further support buoyancy-driven flow as a viable mechanism for rapid exhumation of these deep rocks. To understand how these domes develop in orogens requires addressing the general question of partial melting during orogenesis. In this chapter thus far, we have emphasized the importance of decompression – specifically isothermal decompression – and the tectonic/thermal fate of partially molten crust. We have focused on relatively small- (crustal-) scale observations, but will now consider larger- (lithosphere-) scale processes that might contribute to melting of continental crust. By doing so, we can address the fundamental question of how and why the deep crust of orogens attains such high melt fractions over such a great crustal thickness (Nelson *et al.* 1996; Schilling & Partzsch 2001).

Buoyant return of subducted continental crust

The contribution of continental subduction to melting in orogens requires further consideration. In the mid- to deep crust of the southern Tibetan Plateau, it is difficult to explain the presence of the amount of melt inferred (20 vol.%) by simple heating during crustal shortening, as the mantle is not unusually hot beneath this part of Tibet (Nelson *et al.* 1996; Chen *et al.* 1996). In addition, the rapid rate of underthrusting (subduction) of Indian crust beneath Eurasia (55–60 mm a^{-1}; Patriat & Achache 1984; Le Pichon *et al.* 1992) and the estimated low temperature at the Indian plate moho at the modern suture (inferred from heat flow data; Gupta 1993) suggest that the lower crust of the subducting Indian continent is at moderate temperatures (<800 °C; Henry *et al.* 1997). Nelson *et al.* (1996) proposed that crustal heat production in 70 km thick continental crust caused partial melting in the Tibetan crust. This mechanism, however, requires the presence of a free aqueous fluid for flux melting, and this combination of variables (enough time for heat production to promote regional-scale melting, the presence of abundant aqueous fluids) is unlikely. However, decompression due to thinning, extension, or buoyant rise of deep crust (including subducted Indian or Eurasian continental material)

(Fig. 3) may account for large degrees of melting without the presence of water-rich fluid and without the presence of elevated temperatures (i.e. >800 °C).

The UHP terranes identified at the Earth's surface represent a small fraction of the total volume of subducted continental material. For example, the amount of Indian continental crust that is estimated to have been buried/subducted beneath the Eurasian plate cannot be accounted for by the amount of crustal thickening in the Himalayas. Some of the missing crust has likely flowed under southern Tibet. Although some subducted continental crust may become dense enough to sink into the mantle as eclogite (Le Pichon *et al.* 1992), some crust may remain less dense than the surrounding mantle rocks (Hermann 2002) and can rise buoyantly. The question of the fate of subducted continental crust is related to the present discussion because the buoyant rise of subducted continental crust may contribute to partial melting in collisional orogens, by providing source rocks for partial melting during decompression and/or by influencing decompression mechanisms in the overlying (non-subducting) crust.

It is unclear at present whether exhumed UHP rocks were partially melted during ultrahigh-pressure metamorphism. Some UHP terranes contain abundant migmatites (e.g. Dabie Shan), but the general view is that the partial melting occurred in a later event, unrelated to UHP metamorphism (Coleman & Wang 1995). Furthermore, geochemical studies in some exhumed ultrahigh-pressure terranes suggest that the continental material was 'old, cold, and dry' (Coleman & Wang 1995) prior to subduction. Sharp *et al.* (1993), however, proposed that the stable isotope values of UHP schists from the Dora Maira Massif indicated equilibration with a melt, possibly represented by kyanite + jadeite + garnet + quartz layers in the schists (Schreyer *et al.* 1987). We believe the relationships among UHP metamorphism, exhumation of UHP rocks and partial melting deserve further investigation, but, whether or not exhumed UHP terranes experienced partial melting, it is reasonable to propose that some subducted continental material has sufficient fertility and reaches P-T conditions appropriate for partial melting during deep subduction and/or decompression.

Summary

Large-magnitude (>10 km), regional-scale decompression that is nearly isothermal at elevated temperatures (>700 °C) may be driven by a variety of mechanisms, including surficial and deep crust/mantle processes that may influence each other through feedback relationships. If decompression is a necessary condition for large-scale melting of continental crust, then a significant source of material and/or a major driving force for melting in collisional orogens may be subducted continental material. The transfer of continental material, including melt, from the subducting plate to the non-subducting plate may result in decompression-driven partial melting, with the melt accumulating in the non-subducting plate. The large volume of melt in a layer within the thickened crust fundamentally changes the balance between tectonic and buoyancy forces in a collisional orogen and results in mechanical decoupling of continental crust and lithospheric mantle. Within continental crust, upper and deep levels may initially be mechanically coupled (e.g. if decompression is driven by surficial or other upper crustal processes), but these too become decoupled through time as partial melting proceeds and the deep crust flows laterally (channel flow) and/or vertically (diapirism). The rise of partially molten crust and associated downflow of denser country rocks signifies decoupling of orogenic crust from the mantle lithosphere and of deep crust from upper crust.

We thank Olivier Vanderhaeghe for his comments on the paper, and acknowledge reviews by Mike Brown and J.-L. Vigneresse. In particular, the helpful suggestions of Mike Brown improved the discussion of migmatites and melting relationships. This work was partially supported by NSF grant EAR-9814669.

References

AUDREN, C. & TRIBOULET, C. 1993. *P–T–t* deformation paths recorded by kinzigites during diapirism in the western Variscan belt (Golfe du Morbihan, southern Brittany, France). *Journal of Metamorphic Geology*, **11**, 337–356.

BEAUMONT, C., JAMIESON, R.A., NGUYEN, M.H & LEE, B. 2001. Himalayan tectonics explained by extrusion of a low-viscosity crustal channel coupled to focused surface denudation. *Nature*, **414**, 738–742.

BERNER, H., RAMBERG, H. & STEPHANSSON, O. 1972. Diapirism in theory and experiment. *Tectonophysics*, **15**, 197–218.

BROWN, L.D., ZHAO, W. *et al.* 1996. Bright spots, structure, and magmatism in Southern Tibet from INDEPTH seismic reflection profiling. *Science*, **274**, 1688–1690.

BROWN, M. 1979. The tectonic evolution of the Precambrian rocks of the St. Malo region, Armorican Massif, France. *Precambrian Research*, **6**, 1–21.

BROWN, M. 1994. The generation, segregation, ascent and emplacement of granite magma; the

migmatite-to-crustally-derived granite connection in thickened orogens. *Earth Science Reviews*, **36**, 83–130.

BROWN, M. & DALLMEYER, R.D. 1996. Rapid Variscan exhumation and the role of magma in core complex formation; southern Brittany metamorphic belt, France. *Journal of Metamorphic Geology*, **14**, 361–379.

BROWN, M. & SOLAR, G.S. 1998. Shear zone systems and melts: feedback relations and self-organization in orogenic belts. *Journal of Structural Geology*, **20**, 211–227.

BRUN, J.-P. & VAN DEN DRIESSCHE, J. 1994. Extensional gneiss domes and detachment faults – structure and kinematics. *Bulletin of the Geological Society of France*, **165**, 519–530.

BUCK, W.R., 1988. Flexural rotation of normal faults. *Tectonics*, **7**, 959–973.

BURG, J.-P. & PODLADCHIKOV, Y. 2000. From buckling to asymmetric folding of the continental lithosphere; numerical modelling and application to the Himalayan syntaxes. *In*: KHAN, M.A., TRELOAR, P.J., SEARLE, M.P. & JAN, M.Q. (eds), *Tectonics of the Nanga Parbat Syntaxis and the Western Himalaya*, Geological Society, London, Special Publications, **170**, 219–236.

BURG, J.-P., GUIRAUD, M., CHEN, G.M. & LI, G.C. 1984. Himalayan metamorphism and deformations in the north Himalayan Belt (southern Tibet, China). *Earth and Planetary Science Letters*, **69**, 391–400.

BURG, J.P., DAVY, P. & MARTINOD, J. 1994. Shortening of analogue models of the continental lithosphere; new hypothesis for the formation of the Tibetan Plateau. *Tectonics*, **13**, 475–483.

BURG, J.-P., DAVY, P., NIEVERGELT, P., OBERLI, F., SEWARD, D., DIAO, Z. & MEIER, M. 1997. Exhumation during crustal folding in the Namche–Barwa syntaxis. *Terra Nova*, **9**, 53–56.

CALVERT, A., GANS, P.B. & AMATO, J.M. 1999. Diapiric ascent and cooling of a sillimanite gneiss dome revealed by $^{40}Ar/^{39}Ar$ thermochronology: the Kigluaik Mountains, Seward Peninsula, Alaska: In: RING, U., BRANDON, M.T., LISTER, G.S. & WILLETT, S.D. (eds) *Exhumation Processes: Normal Faulting, Ductile Flow, and Erosion.* Geological Society, London, Special Publications, **154**, 205–232.

CHEMENDA, A.I., MATTAUER, M., MALAVIEILLE, J. & BOKUN, A.N. 1995. A mechanism for syn-collisional deep rock exhumation and associated normal faulting: results from physical modeling. *Earth and Planetary Science Letters*, **132**, 225–232.

CHEN, L., BOOKER, J.R., JONES, A.G., WU, N., UNSWORTH, M.J., WEI, W. & TAN, H. 1996. Electrically conductive crust in southern Tibet from INDEPTH magnetotelluric surveying. *Science*, **274**, 1694–1696.

CHEN, Z., LIU, Y., HODGES, K.V., BURCHFIEL, B.C., ROYDEN, L.H & DENG, C. 1990. The Kangmar Dome: a metamorphic core complex in southern Xizang (Tibet). *Science*, **250**, 1552–1556.

CHOPIN, C. 1984. Coesite and pure pyrope in high-grade blueschists of the western Alps: a first record and some consequences. *Contributions to Mineralogy and Petrology*, **86**, 107–118.

CLEMENS, J.D & MAWER, C.K. 1992. Granitic magma transport by fracture propagation. *Tectonophysics*, **204**, 339–360.

CLEMENS, J.D. & VIELZEUF, D. 1987. Constraints on melting and magma production in the crust. *Earth and Planetary Science Letters*, **86**, 287–306.

COLEMAN, R.G. & WANG, X. 1995. *Ultrahigh-Pressure Metamorphism*. Cambridge University Press, New York.

DUNN, S.R. & MEDARIS, L.D. 1989. Retrograded eclogites in the Western Gneiss region of a portion of the Scandinavian Caledonides. *Lithos*, **22**, 229–245.

ENGLAND, P.C. & THOMPSON, A.B. 1984. Pressure–temperature–time paths of regional metamorphism. I. Heat transfer during the evolution of regions of thickened continental crust. *Journal of Petrology*, **25**, 894–928.

ENGLAND, P.C. & THOMPSON, A.B. 1986. Some thermal and tectonic models for crustal melting in continental collision zones. *In*: COWARD, M.P. & RIES, A.C. (eds) *Collision Tectonics.* Geological Society, London, Special Publications, **19**, 83–94.

ESCUDER VIRUETE, J., INDARES, A. & ARENAS, R., 2000. *P–T* paths derived from garnet growth zoning in an extensional setting: an example from the Tormes Gneiss Dome (Iberian Massif, Spain). *Journal of Petrology*, **41**, 1489–1515.

ESKOLA, P.E. 1949. The problem of mantled gneiss domes. *Quarterly Journal of the Geological Society, London*, **104**, 461–476.

FAYON, A.K., WHITNEY, D.L. & TEYSSIER, C. 2002. Isothermal decompression of migmatites: diapirism or normal faulting? *Geological Society of America Abstracts with Programs*, **34**, 333.

FLETCHER, R.C. 1972. Application of a mathematical model to the emplacement of mantled gneiss domes. *American Journal of Science*, **272**, 197–216

GERBAULT, M. 2000. At what stress level is the central Indian Ocean lithosphere buckling? *Earth and Planetary Science Letters*, **178**, 165–181.

GRUJIC, D., HOLLISTER, L.S. & PARRISH, R.R. 2002. Himalayan metamorphic sequence as an orogenic channel: insight from Bhutan. *Earth and Planetary Science Letters*, **198**, 177–191.

GUPTA, M.L. 1993. Is the Indian shield hotter than other Gondwana shields? *Earth and Planetary Science Letters*, **115**, 275–285.

HENRY, P., LE PICHON, X. & GOFFE, B. 1997. Kinematic, thermal, and petrological model of the Himalayas: constraints related to metamorphism within the underthrust Indian crust and topographic elevation. *Tectonophysics*, **273**, 31–56.

HERMANN, J. 2002. Experimental constraints on phase relations in subducted continental crust. *Contributions to Mineralogy and Petrology*, **43**, 219–235.

HIRN, A., SAPIN, M., LEPINE, J.C., DIAZ, J. & MEI, J. 1997. Increase in melt fraction along a south–north traverse below the Tibetan Plateau: evidence from seismology. *Tectonophysics*, **273**, 17–30.

HOLLOWAY, J.R. & BLANK, J.G. 1994. Application of experimental results to C–O–H species in natural melts. *In*: CARROLL, M.R. & HOLLOWAY, J.R. (eds) Volatiles in Magmas. *Reviews in Mineralogy*, **30**, 187–230.

INGER, S. & HARRIS, N. 1993. Geochemical constraints on leucogranite magmatism in the Langtang Valley, Nepal, Himalaya. *Journal of Petrology*, **34**, 345–368.

JONES, K.A. & BROWN, M. 1990. High-temperature 'clockwise' *P–T* paths and melting in the development of regional migmatites: an example from southern Brittany, France. *Journal of Metamorphic Geology*, **8**, 551–578.

LEE, J., HACKER, B.R. *et al.* 2000. Evolution of the Kangmar Dome, southern Tibet: structural, petrologic, and thermochronologic constraints. *Tectonics*, **19**, 872–895.

LE FORT, P., CUNEY, M., DENIEL, C., FRANCE-LANORD, C., SHEPPARD, S.M.F., UPRETTI, B.N. & VIDAL, P. 1987. Crustal generation of the Himalayan leucogranites. *Tectonophysics*, **134**, 39–57.

LE PICHON, X., FOURNIER, M. & JOLIVET, L. 1992. Kinematics, topography, shortening, and extrusion in the India–Eurasia collision. *Tectonics*, **11**, 1085–1098.

LISTER, G.A. & DAVIS, G.A. 1989. The origin of metamorphic core complexes and detachment faults formed during Tertiary continental extension in the northern Colorado River region, U.S.A. *Journal of Structural Geology*, **11**, 65–94.

MARTINOD, J. & DAVY, P. 1994. Periodic instabilities during compression of the lithosphere; 2, Analogue experiments. *Journal of Geophysical Research*, **99**, 12057–12069.

MCKENZIE, D. 1984. The generation and compaction of partially molten rocks. *Journal of Petrology*, **25**, 713–765.

MONTEL, J.M., MARIGNAC, C., BARBEY, P. & PICHAVANT, M. 1992. Thermobarometry and granite genesis: the Hercynian low-*P* high-*T* Velay anatectic dome (French Massif Central). *Journal of Metamorphic Geology*, **10**, 1–15.

NAKAMURA, D. & HIRAJAMA, T. 2000. Granulite-facies overprinting of ultrahigh-pressure metamorphic rocks, northeastern Su-Lu region, Eastern China. *Journal of Petrology*, **41**, 563–582.

NELSON, K.D., ZHAO, W. *et al.* 1996. Partially molten middle crust beneath southern Tibet: synthesis of Project INDEPTH results. *Science*, **274**, 1684–1688.

NORLANDER, B.N., WHITNEY, D.L., TEYSSIER, C. & VANDERHAEGHE, O. 2002. Partial melting and decompression of the Thor-Odin dome, Shuswap metamorphic core complex, Canadian Cordillera. *Lithos*, **61**, 103–125.

NOYE, J. 1982, Finite difference method for partial differential equations. *In*: NOYE, J. (ed.) *Numerical Solutions of Partial Differential Equations.* North-Holland, Amsterdam, 3–137.

NYMAN, M.W., PATTISON, D.R.M. & GHENT, E.D. 1995. Melt extraction during formation of K-feldspar + sillimanite migmatites, west of Revelstoke, British Columbia. *Journal of Petrology*, **36**, 351–372.

OWENS, T.J. & ZANDT, G. 1997. Implications of crustal property variations for models of Tibetan Plateau evolution. *Nature*, **387**, 37–53.

PATRIAT, P. & ACHACHE, J. 1984. India–Asia collision chronology and implications for crustal shortening and driving mechanisms of plates. *Nature*, **311**, 615–621.

POUS, J., MUÑOZ, J.A., LEDO, J.J. & LIESA, M. 1995. Partial melting of subducted continental lower crust in the Pyrenees. *Journal of the Geological Society, London*, **152**, 217–220.

RAMBERG, H. 1980. Diapirism and gravity collapse in the Scandinavian Caledonides. *Journal of the Geological Society, London*, **137**, 261–270.

RAMSAY, J.G. 1967. *Folding and Fracturing of Rocks.* McGraw-Hill, New York.

REY, P. 1993. Seismic and tectonometamorphic characters of the lower continental crust in Phanerozoic areas: a consequence of post-thickening extension. *Tectonics*, **12**, 580–590.

ROLLAND, Y., MAHÉO, G., GUILLOT, S. & PÊCHER, A. 2001. Tectono-metamorphic evolution of the Karakorum Metamorphic complex (Dassu–Askole area, NE Pakistan): exhumation of mid-crustal HT-MP gneisses in a convergent context. *Journal of Metamorphic Geology*, **19**, 717–737.

SAWYER, E.W. 2001. Melt segregation in the continental crust: distribution and movement of melt in anatectic rocks. *Journal of Metamorphic Geology*, **19**, 291–309.

SCHILLING, F.R. & PARTZSCH, G.M. 2001. Quantifying partial melt fraction in the crust beneath the central Andes and the Tibetan Plateau. *Physics and Chemistry of the Earth*, **26**, 239–246.

SCHREYER, W., MASSONE, H.-J. & CHOPIN, C. 1987. Continental crust subducted to depths near 100 km: implications for magma and fluid genesis in collision zones. *In*: MYSEN, B.O. (ed.) *Magmatic Processes: Physicochemical Principles.* Geochemical Society Special Publication, **1**, 155–163.

SEARLE, M., HACKER, B.R. & BILHAM, R. 2001. The Hindu Kush seismic zone as a paradigm for the creation of ultrahigh-pressure diamond- and coesite-bearing continental rocks. *Journal of Geology*, **109**, 143–153.

SHARP, Z.D., ESSENE, E.J. & HUNZIKER, J.C. 1993. Stable isotope geochemistry and phase equilibria of coesite-bearing whiteschists, Dora Maira Massif, western Alps. *Contributions to Mineralogy and Petrology*, **114**, 1–12.

Soula, J.-C., DEBAT, P., BRUSSET, S., BESSIER, G., CHRISTOPHOUL, F. & DERAMOND, J. 2001. Thrust-related, diapiric, and extensional doming in a frontal orogenic wedge: example of the Montagne Noire, Southern French Hercynian Belt. *Journal of Structural Geology*, **23**, 1677–1699.

TAPPONNIER, P., ZHIQIN, X., ROGER, F., MEYER, B., ARNAUD, N., WITTLINGER, G. & JINGSUI, Y. 2001. Oblique stepwise rise and growth of the Tibetan Plateau. *Science*, **294**, 1671–1677.

TEYSSER, C. & WHITNEY, D.L. 2002. Gneiss domes and orogeny. *Geology*, **30**, 1139–1142.

THOMPSON, A.B. 2000. Clockwise *P–T* paths for crustal melting and H_2O recycling in granite source regions and migmatite terrains. *Lithos*, **56**, 33–35.

VANDERHAEGHE, O., TEYSSIER, C. & WYSOCZANSKI, R. 1999. Structural and geochronological constraints on the role of partial melting during the formation of the Shuswap metamorphic core complex at the latitude of the Thor-Odin Dome, British Columbia. *Canadian Journal of Earth Sciences*, **36**, 917–943.

VAN DER VOO, R., SPAKMAN, W. & BIJWAARD, H. 1999. Tethyan subducted slabs under India. *Earth and Planetary Science Letters*, **171**, 7–20.

VIELZEUF, D. & HOLLOWAY, J.R. 1988. Experimental determination of the fluid-absent melting relations in the pelitic system. Consequences for crustal differentiation. *Contributions to Mineralogy and Petrology*, **98**, 257–276.

WANG, Q., ISHIWATARI, A., *et al.* 1993. Coesite-bearing granulite retrograded from eclogite in Weihai, eastern China. *European Journal of Mineralogy*, **5**, 141–152.

WHITNEY, D.L. 1992. High pressure metamorphism in the western Cordillera of North America: an example from the Skagit Gneiss, North Cascades, Washington. *Journal of Metamorphic Geology*, **10**, 71–85.

WHITNEY, D.L. & IRVING, A.J. 1994. Origin of K-poor leucosomes in a metasedimentary migmatite complex by ultrametamorphism, syn-metamorphic magmatism, and subsolidus processes. *Lithos*, **32**, 173–192.

WICKHAM, S. 1987. Crustal anatexis and granite petrogenesis during low-pressure regional metamorphism; the Trois Seigneurs Massif, Pyrenees, France. *Journal of Petrology*, **28**, 127–169.

WIESSEL, J.K., ANDERSON, R.N. & GELLER, C.A. 1980. Deformation of the Indo-Australian plate, *Nature*, **87**, 284–291.

ZEITLER, P.K., KOONS, P.O. *et al.* 2001. Crustal reworking at Nanga Parbat, Pakistan. Metamorphic consequences of thermal-mechanical coupling facilitated by erosion. *Tectonics*, **20**, 712–728.

ZHANG, R.Y., LIOU, J.G., ERNST, W.G., COLEMAN, R.G., SOBOLEV, N.V. & SHATSKY, V.S. 1997. Metamorphic evolution of diamond-bearing and associated rocks from the Kokchetav Massif, northern Kazakhstan. *Journal of Metamorphic Geology*, **15**, 479–496.

ZHAO, W., NELSON, K.D. *et al.* 1993. Deep seismic reflection evidence for continental underthrusting beneath southern Tibet. *Nature*, **366**, 557–559.